Pergamon

Int. J. Heat Mass Transfer. Vol. 39, No. 13, pp. 2671–2681, 1996

0017-9310/96 $15.00+0.00

0017-9310(95)00350-9

Cooperating thermosolutal convection in enclosures—I. Scale analysis and mass transfer

R. BENNACER† and D. GOBIN

Fluides, Automatique et Systèmes Thermiques, URA 871, Laboratoire de l'Université Pierre et Marie Curie associé au CNRS, Campus Universitaire, Bât. 502. 91405 Orsay Cedex, France

(*Received* 27 *January* 1995 *and in final form* 26 *September* 1995)

Abstract—This paper reports the analytical and numerical results on double diffusive natural convection in a binary fluid contained in a two-dimensional enclosure where horizontal temperature and concentration differences are specified. A numerical code, based on a finite volume procedure, and a scaling law approach are used to analyse the influence of the different parameters which characterize those thermosolutal flows: in this first paper, the mass transfer problem is studied in the steady-state. A general mass transfer correlation is proposed, which is valid over a wide range of parameters. Copyright © 1996 Elsevier Science Ltd.

1. INTRODUCTION

Thermosolutal natural convection is present in many industrial processes, especially those involving phase change phenomena (melting or solidification). For instance, the growth of a solid phase from a binary melt due to a temperature gradient causes solute redistribution at the solidification front and the composition of the liquid phase undergoes local changes. The subsequent density gradient combines to the thermal effect and a two component buoyancy force is induced in the fluid.

The bibliography reveals a great number of studies on double diffusion convection, due to the industrial or technological importance of the fields of application (materials processing, oceanography, as reported by Chen and Johnson [1]). Three main configurations have been considered in the previous works:

(1) double diffusion in an horizontal layer with vertical temperature and concentration gradients;
(2) sideways heating of an initially stratified fluid layer;
(3) thermosolutal natural convection due to horizontal temperature and concentration gradients.

The present study is concerned with this latter situation. In this field, the early analytical studies have been mainly dedicated to the analysis of limited problems: either the Lewis number is of order 1, as in the asymptotic methods proposed by Saville and Churchill [2], or Gebhart and Pera [3], or one component of the buoyancy term is dominating, as in the analytical approach by Bejan [4] which leads to the scaling laws in the heat transfer driven or mass transfer driven regimes.

The main studies on thermosolutal natural convection in enclosures may be classified according to the order of magnitude of the Lewis number (Le = thermal diffusivity/molecular diffusivity). The range of low and moderate Le numbers ($Le \sim 1$–10) refers to double diffusion in binary gases. Few experiments are available [5], but many numerical results have been published, because the numerical problem is close to the thermal convection problem. The high Lewis number domain (Le of order 10^2 and more) is related to thermosolutal convection in liquids: it leads to more complex situations in terms of heat and mass transfer, and to more interesting challenges from both the numerical and the experimental standpoints.

During the last 10 years, a number of experimental and analytical studies have dealt with situations where the temperature and concentration boundary conditions are specified at the vertical walls of a confined cavity. The experimental studies generally use aqueous solutions (NaCl, Na_2CO_3 or $CuSO_4$ solutions), corresponding to a Prandtl number of 7, and to a Lewis number of order 200 [6–9]. Experimentally, the main problem is to impose uniform and constant concentrations at a wall. Lee *et al.* [7] used membranes to separate the cell containing the working binary fluid from the regulated temperature and concentration baths. Kamotani *et al.* [6] and Han and Kuehn [8] developed an electrochemical technique to impose the concentrations at the copper heat exchangers used as electrodes. In reality, the spatial uniformity of the wall concentration has not been verified and the mean value is proved to change with time. The conclusions of these studies are thus limited.

The first numerical simulations and analytical calculations of thermosolutal natural convection in enclosures due to horizontal temperature and con-

† Present address: IUSI, rue d'Eragny, 95031 Neuville-sur-Oise, France.

NOMENCLATURE

A	aspect ratio of the enclosure, H/L
C	dimensional concentration
D	mass diffusivity
g	intensity of gravity
Gr_S	solutal Grashof number based on $H, g\beta_S\Delta CH^3/\nu^2$
Gr_T	thermal Grashof number based on $H, g\beta_T\Delta TH^3/\nu^2$
$H(L)$	height (width) of the enclosure
$\mathbf{i}(\mathbf{k})$	unit vector in the horizontal (vertical) direction
k	thermal conductivity
Le	Lewis number: Sc/Pr
N	buoyancy ratio: Gr_S/Gr_T
$\overline{Nu}$	average Nusselt number (dimensionless heat flux)
P	dimensionless pressure
Pr	Prandtl number, ν/α
Sc	Schmidt number, ν/D
$\overline{Sh}$	average Sherwood number (dimensionless mass flux)
T	dimensional temperature
$u(w)$	horizontal (vert.) dimensionless component of velocity
$\mathbf{V}^*$	dimensional velocity
$\mathbf{V}$	dimensionless velocity
w_S	vertical velocity scale on the solutal boundary layer scale
w_T	vertical velocity scale on the thermal boundary layer scale
$x^*(z^*)$	dimensional horizontal (vertical) coordinate
$x(z)$	dimensionless coordinate, $x^*/H(z^*/H)$.

Greek symbols

α	thermal diffusivity
β_T	coefficient of volumetric expansion with temperature
β_S	coefficient of volumetric expansion with concentration
ΔC	concentration difference between plates, C_2-C_1
ΔT	temperature difference between plates, T_2-T_1
δ_T	thermal boundary layer thickness
δ_S	solutal boundary layer thickness
ν	kinematic viscosity
μ	viscosity
ϕ	dimensionless concentration: $(C-(C_2+C_1)/2)/\Delta C$
ρ	fluid density
θ	dimensionless temperature: $(T-(T_2+T_1)/2)/\Delta T$.

Subscripts

0	reference
1	hot side
2	cold side
eq.	equivalent
H	based on H
S	solutal
T	thermal.

centration gradients at moderate values of the Lewis number are proposed by Trevisan and Bejan [10], Ranganathan and Viskanta [11], Bénard *et al.* [12], Lee and Hyun [13], Weaver and Viskanta [5] and Béghein *et al.* [14]. Most studies are concerned with Lewis numbers close to 1, which considerably limit the scope of the results. Indeed, the problem of thermosolutal convection at $Le = 1$ is identical to the classical problem of thermal natural convection, with an effective Grashof number resulting from the addition of the thermal and solutal Grashof numbers. Partial numerical results considering high Lewis numbers have been obtained by Han and Kuehn [8] and Shyy and Chen [15].

The symmetry of the boundary conditions applied at the vertical walls allows for the existence of a steady-state solution. Nevertheless, in the opposing case, the observations show that, under some conditions, non-stationary or fluctuating behaviours may be found [16, 17].

Among the aforementioned studies, a few papers indicate the existence of multicellular flow structures [18], but the theoretical prediction of the transition from a monocellular to a multicellular regime has still to be discussed. This aspect is presented in the companion paper. Concerning the heat and mass transfer characteristics, orders of magnitude have been proposed by Bejan in the extreme situations where either the thermal or the solutal effect is dominating the flow [4], and no general expression for the Nusselt or Sherwood numbers is available over a wide range of parameters.

The present study will be mainly dedicated to steady-state solutions for cooperating buoyancy forces (the thermal and solutal terms act in the same direction). This restriction is due to the non-stationarity that may appear in the opposing situation, as mentioned by several experimental studies [6, 9, 16]. Also, only the case of fluids presenting a Prandtl number larger than unity will be considered (for the $Pr < 1$ range, the reader may refer to the study by Shyy and Chen [15]), with a Lewis number $Le \gg 1$, which corresponds mainly to liquids.

Our objective is to complete the numerical results

that have been presented on the influence of the main parameters Gr_T, N and Le on the average wall Sherwood and Nusselt numbers, in order to verify the orders of magnitude and to present some global correlations on a wide range of parameters. This study is presented in two papers: the first part is dedicated to the analysis of the influence of the governing parameters on the mass transfer, and a study of the orders of magnitude of the leading terms is compared to the numerical results. The companion paper is concerned with heat transfer and flow structure, particularly of the multicellular flow regimes that may appear in such systems.

2. PROBLEM DEFINITION

Let us consider a two-dimensional rectangular cavity (height H, width L, aspect ratio $A = H/L$) where different, but uniform temperatures and concentrations are specified at the two vertical walls T_1 and T_2 (C_1 and C_2), respectively. Zero heat and mass flux are assumed at the top and bottom walls of the enclosure, and no-slip dynamic boundary conditions are imposed at the walls (Fig. 1).

In this study, the main usual hypotheses of incompressible and laminar flow are considered. The binary fluid is assumed to be Newtonian and its density is supposed to be constant, except in the driving term of the Navier–Stokes equation, where it varies linearly with the local temperature and solute mass fraction

$$\rho(T,C) = \rho_0[1-\beta_T(T-T_0)-\beta_S(C-C_0)] \quad (1)$$

with $\beta_T > 0$ and $\beta_S < 0$, and $\Delta\rho/\rho < 0.1$, assuming

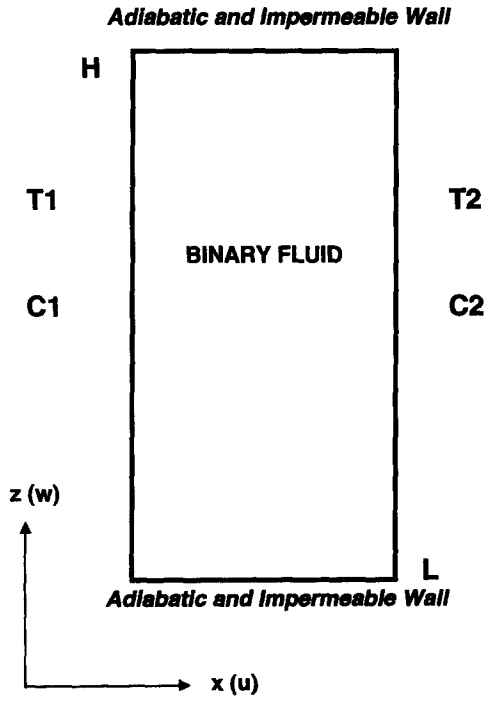

Fig. 1. Schematic representation of the problem under study.

that the Oberbeck–Boussinesq approximation may be used. The thermophysical properties of the fluid are taken as constants, and they are estimated at a reference temperature T_0 and solute mass fraction C_0. Viscous dissipation and radiative heat transfer are not considered, and the Soret and Dufour effects are neglected. The corresponding set of governing equations is, in dimensional terms

Continuity equation

$$\nabla\cdot\mathbf{V}^* = 0 \quad (2)$$

Energy conservation equation

$$\frac{\partial T}{\partial t^*} + \mathbf{V}^*\cdot\nabla^* T = \alpha\Delta^* T \quad (3)$$

Species conservation equation

$$\frac{\partial C}{\partial t^*} + \mathbf{V}^*\cdot\nabla^* C = D\Delta^* C \quad (4)$$

Momentum equation

$$\rho_0\left(\frac{\partial \mathbf{V}^*}{\partial t^*} + (\mathbf{V}^*\cdot\nabla^*)\mathbf{V}^*\right) = \mu\nabla^{*2}\mathbf{V}^* - \nabla^* P^* - \rho g\mathbf{k} \quad (5)$$

where P^* is the pressure and g is the intensity of gravity.

Equations (2)–(5) may be expressed in terms of the reduced velocity, temperature and concentration, $\mathbf{V}$, θ and ϕ, defined as

$$\mathbf{V} = \frac{H}{\nu}\mathbf{V}^* \quad \theta = \frac{(T-T_0)}{\Delta T} \quad \phi = \frac{(C-C_0)}{\Delta C} \quad (6)$$

with $T_0 = (T_1+T_2)/2$, $\Delta T = (T_2-T_1)$,
and $C_0 = (C_1+C_2)/2$, $\Delta C = (C_2-C_1)$.

This leads to the following dimensionless conservation equations:

$$\nabla\cdot\mathbf{V} = 0 \quad (7)$$

$$\frac{\partial\theta}{\partial t} + \mathbf{V}\cdot\nabla\theta = \frac{1}{Pr}\Delta\theta \quad (8)$$

$$\frac{\partial\phi}{\partial t} + \mathbf{V}\cdot\nabla\phi = \frac{1}{Sc}\Delta\phi \quad (9)$$

$$\frac{\partial\mathbf{V}}{\partial t} + (\mathbf{V}\cdot\nabla)\mathbf{V} = \nabla^2\mathbf{V} - \nabla P + (Gr_T\theta + Gr_S\phi)\mathbf{k}. \quad (10)$$

The parameters of the problem are the aspect ratio of the enclosure ($A = H/L$), and the classical dimensionless numbers of thermal natural convection, the Grashof and the Prandtl number

$$Gr_T = \frac{g\beta_T\Delta T H^3}{\nu^2}, \quad Pr = \frac{\nu}{\alpha} \quad (11)$$

and the corresponding parameters for mass transfer: the solutal Grashof number and the Schmidt number

$$Gr_S = \frac{g\beta_S \Delta C H^3}{\nu^2}, \quad Sc = \frac{\nu}{D}. \tag{12}$$

Two important dimensionless groups, defined as combinations of these parameters, will be used later

(1) the buoyancy ratio

$$N = \frac{Gr_S}{Gr_T} = \frac{\beta_S \Delta C}{\beta_T \Delta T},$$

(2) the Lewis number:

$$Le = \frac{Sc}{Pr} = \frac{\alpha}{D}.$$

The dimensionless boundary conditions resulting from the hypotheses are

$$x = 0: \quad \theta = 0.5 \quad \phi = 0.5 \quad u = w = 0 \tag{13}$$

$$x = 1/A: \quad \theta = -0.5 \quad \phi = -0.5 \quad u = w = 0 \tag{14}$$

$$z = 0 \quad z = 1: \quad \frac{\partial \theta}{\partial z} = 0 \quad \frac{\partial \phi}{\partial z} = 0 \quad u = w = 0. \tag{15}$$

The dimensionless expressions defining the heat and mass fluxes are obtained using a diffusive reference flux ($k\Delta T/H$ for heat transfer, $D\Delta C/H$ for mass transfer). The average values in a vertical plane are:

(1) the Nusselt number

$$\overline{Nu} = \int_0^1 (Pr\, u\theta + \partial\theta/\partial x)\, dz$$

(2) the Sherwood number

$$\overline{Sh} = \int_0^1 (Sc\, u\phi + \partial\phi/\partial x)\, dz.$$

3. SCALING LAWS

The purpose of the present section is to analyse the orders of magnitude of the different terms governing heat and mass transfer in such a system. In a reference work, Bejan [4] uses the vertical boundary layer approximation to extend the scaling analysis of natural convective flows in enclosures to the problem of double diffusion; the analysis is performed in the extreme situations where either the thermal or the solutal component of the buoyancy force is dominant. This section is dedicated to the determination of the limits of validity of the corresponding scaling laws, and to their extension to the intermediate zone where both the thermal and the solutal contributions appear in the buoyancy term. The foregoing analysis is limited to the cooperating situation ($N > 0$) for liquids ($Le \gg 1$) in the $Pr > 1$ domain.

3.1. *Dominating thermal buoyancy term*

This situation is characterized by $|\beta_T \Delta T| \gg |\beta_S \Delta C|$ in equation (1), meaning that solute advection is due to a convective flow which is imposed by the density variation corresponding to the thermal conditions, and that it is not significantly affected by the concentration gradients. Thus, the orders of magnitude of *thermal natural convection* [4] may be applied to δ_T—the thermal boundary layer thickness, and w_T—the vertical velocity scale

$$\begin{cases} \delta_T \sim H Ra_T^{-1/4} \\ w_T \sim \dfrac{\alpha}{H} Ra_T^{1/2} \end{cases} \tag{16}$$

where the thermal Rayleigh number

$$\left(Ra_T = \frac{g\beta_T \Delta T H^3}{\alpha \nu} \right)$$

is based on the height H of the enclosure. Note that expressions (16) are valid in the $Pr \gg 1$ range (the viscous force dominates over inertia, and balances the buoyancy term on the δ_T scale).

The determination of the mass flux results from the study of the solutal boundary layer. Let us define $(\delta_S)_T$ as the solutal boundary layer thickness due to the thermally driven flow; $(\delta_S)_T$ is expected to be smaller than δ_T, since $Le > 1$ [Fig. 2(a)]. Defining $(w_S)_T$ as the vertical fluid velocity induced by the thermal effect on the δ_S scale, it may be assumed that

$$(w_S)_T \sim \frac{(\delta_S)_T}{\delta_T} w_T, \tag{17}$$

and the corresponding orders of magnitude are [4]

$$\begin{cases} (\delta_S)_T \sim H Le^{-1/3} Ra_T^{-1/4} \\ (w_S)_T \sim \dfrac{\alpha}{H} Le^{-1/3} Ra_T^{1/2} \end{cases}. \tag{18}$$

3.2. *Dominating solutal buoyancy term*

In this situation, the same analysis applies to *solutal natural convection* and leads to similar scaling laws, using the solutal Rayleigh number Ra_S instead of Ra_T in equation (16), to determine the solutal boundary layer thickness δ_S and the vertical velocity w_S on the δ_S scale. Noting that $Ra_S = Sc\, Gr_S = Ra_T\, Le\, N$, these expressions may be written [4]

$$\begin{cases} \delta_S \sim H(Ra_T Le\, N)^{-1/4} \\ w_S \sim \dfrac{D}{H}(Ra_T Le\, N)^{1/2} \end{cases}. \tag{19}$$

As previously underlined ($Le > 1$), the thermal boundary layer thickness is larger than δ_S, and the

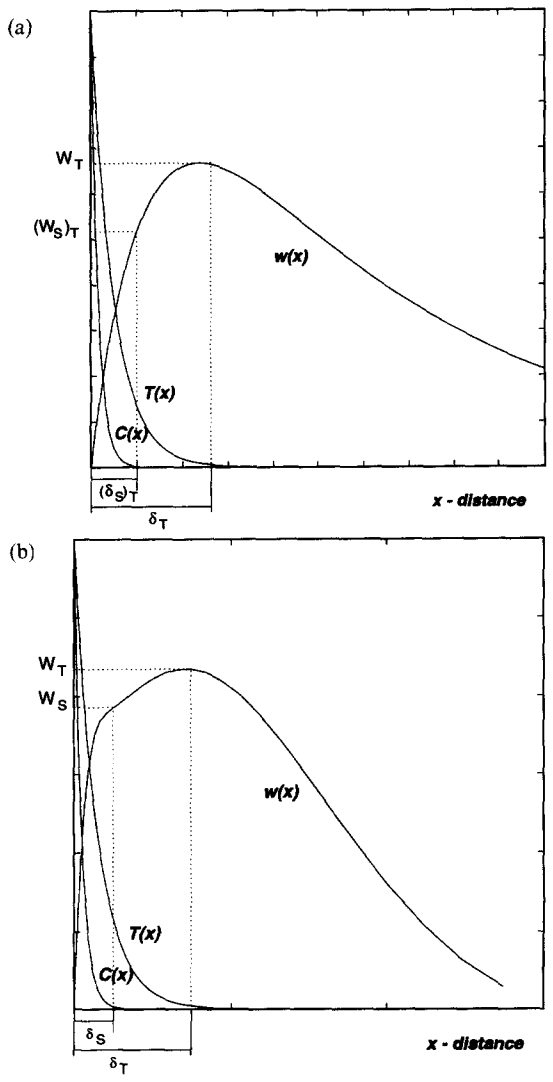

Fig. 2. The boundary layer regime in thermosolutal natural convection: (a) heat transfer dominated flow; (b) dominating mass transfer on the δ_S scale.

temperature variation on the δ_S scale may be considered as small.

After recalling these results, our purpose is to determine the limit of validity of the so-called 'heat transfer driven' and 'mass transfer driven' regimes, and to analyse the heat and mass transfer characteristics in the intermediate regimes.

3.3. *Intermediate zone*

3.3.1. *Mass transfer.* In the heat transfer dominated regime [equation (18)], mass transfer is due to the thermoconvective flow [Fig. 2(a)]. If the solutal buoyancy force is increased at a constant value of Gr_T (increasing N), expressions (19) become valid when the vertical velocity scale (w_S) is one order of magnitude larger than the velocity scale that would be induced by the thermal effect on the same scale ($(w_S)_T$). The condition for a dominant solutal force on the δ_S scale is then

$$w_S \gg (w_S)_T \tag{20}$$

which leads to the conclusion that equation (19) is valid for

$$\frac{N}{Le^{1/3}} \gg 1$$

and that equation (18) may be used when

$$\frac{N}{Le^{1/3}} \ll 1$$

which is in agreement with the criterion used by Bejan [4]. This result implies that, when N is increased from the thermally dominated regime to the compositionally dominated regime, the Sherwood number ($\sim H/\delta_S$) increases from a regime where it does not depend on $N(Sh_T \sim Le^{1/3}Ra_T^{1/4})$ to a regime where it varies as $N^{1/4}(Sh_S \sim (Ra_T Le N)^{1/4})$, with

$$\frac{Sh_S}{Sh_T} = \frac{(\delta_S)_T}{\delta_S} \sim \left(\frac{N}{Le^{1/3}}\right)^{1/4} > 1.$$

3.3.2. *Heat transfer.* From the viewpoint of heat transfer, the two extreme situations described above may be summed up as follows:

(1) If heat transfer is controlled by the thermal buoyancy force, the solutal buoyancy force on the δ_S scale is not sufficient to significantly drive the flow by inertia on the δ_T scale. The velocity scale of the flow due to the solutal force is of order w_S [equation (19)], and a condition for the thermal force to dominate on heat transfer is

$$w_S \ll w_T \tag{21}$$

where w_T is given by equation (16), which leads to

$$\frac{N}{Le} \ll 1. \tag{22}$$

(2) If the solutal buoyancy force on the δ_S scale is strong enough to drive by inertia a flow whose w_S scale is larger than the w_T scale that would be imposed by the thermal buoyancy force, the velocity profile is modified on the δ_T scale and equation (16) cannot be assessed [see Fig. 2(b)]. With the assumption that the scale of the flow velocity on the δ_T scale is of the order of w_S the condition

$$w_S \gg w_T \tag{23}$$

leads to

$$\frac{N}{Le} \gg 1. \tag{24}$$

It is then possible to estimate the order of magnitude in this latter case

$$\delta_T^2 \sim \alpha H/w_S, \text{ with } w_S \sim \frac{D}{H}(Ra_T Le\, N)^{1/2} \quad (25)$$

$$\delta_T \sim H\, Le^{1/4}(Ra_T N)^{-1/4}. \quad (26)$$

It should be noticed that the order of magnitude of δ_T is under-estimated because the velocity on the thermal layer scale—external to the solutal boundary layer—decreases away from the wall, and thus the heat transfer is over-estimated by this approximation. This estimation remains acceptable if the Schmidt number is high enough, because the velocity scale out of δ_S decreases less rapidly.

The conditions that we have determined concerning the value of N/Le allow us to define two domains where heat transfer is dominated by a flow which is induced either by the solutal or by the thermal buoyancy term. In each domain, the scale of the thermal boundary layer thickness and of the vertical velocity component are

$$N/Le \gg 1 \quad \begin{cases} \delta_T \sim H\, Le^{1/4}(Ra_T N)^{-1/4} \\ w_T \sim w_S \sim \dfrac{D}{H}(Ra_T Le\, N)^{1/2} \end{cases},$$

$$N/Le \ll 1 \quad \begin{cases} \delta_T \sim H\, Ra_T^{-1/4} \\ w_T \sim \dfrac{\alpha}{H} Ra_T^{1/2} \end{cases}.$$

The results concerning the orders of magnitude obtained in this section are illustrated in Fig. 3. The previous studies (Bejan [19], Béghein *et al.* [14]) consider that the zones corresponding to the two extreme situations may be defined on the basis of a criterion related to the value of N only: $N \gg 1$ for the 'mass transfer driven regime', or $N \ll 1$ for the 'heat transfer driven regime'. The above analysis shows that the criterion also depends on the Lewis number, through the ratio N/Le for heat transfer and through the group $N/Le^{1/3}$ for mass transfer. This allows us to refine the characterization of the different situations, and the results are in good agreement with the criterion established for porous media [20] and with the inversion condition established by Nilson [21] in the $N < 0$ range.

This figure represents the main zones determined by the scaling analysis. According to the values of N and Le, the mass transfer or heat transfer is dominated by a flow which is mainly due to either the solutal or the thermal buoyancy force:

(1) Zone 1—the thermal buoyancy force is dominating on the δ_T **and** the δ_S scales;

(2) Zone 2—the thermal buoyancy force is dominating on the δ_T scale and the solutal buoyancy force is dominating on the δ_S scale;

(3) Zone 3—the solutal buoyancy force is dominating on the δ_S **and** δ_T scales;

(4) Zone 1′—the thermal buoyancy force is dominating on the δ_T scale, but it cannot be said which term is dominant on the δ_S scale;

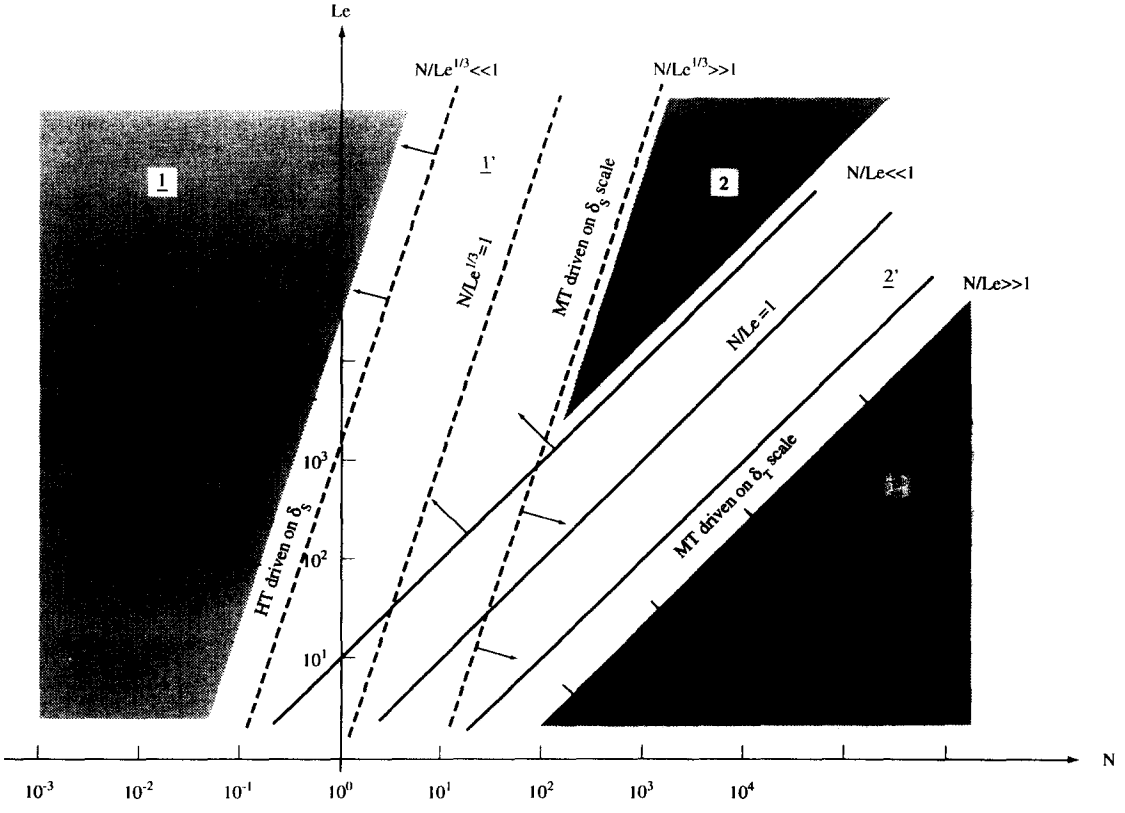

Fig. 3. Sketch of the various situations in the boundary layers.

(5) Zone 2′—the solutal buoyancy force is dominating on the δ_S scale, but it cannot be said which term is dominant on the δ_T scale,

As a first conclusion of this scaling analysis, *in the* $Le > 1$ *and* $Pr > 1$ *domain*, we have shown that:

(1) at low N values ($N \ll Le^{1/3}$), the boundary layer flow is driven by the *thermal* component of the buoyancy term;

(2) with increasing N in the limit $N/Le^{1/3} \gg 1$, the flow on the δ_S scale is driven by the solutal buoyancy term, but if $N/Le \ll 1$ this term is not sufficient to significantly affect the heat transfer on the δ_T scale. In this situation, the ratio of the boundary layer thicknesses $\delta_T/\delta_S \sim (Le\,N)^{1/4}$ confirms the experimental result by Kamotani *et al.* [6];

(3) if N is increased so that $N/Le \gg 1$, the flow driven by the compositional component of the buoyancy term is strong enough to affect the domain at δ_T scale and thus, determines the heat transfer.

4. NUMERICAL RESULTS

4.1. *Numerical model*

The set of coupled equations (7)–(10) governing the fluid flow are solved using a finite volume technique. The numerical procedure is inspired from the classical method proposed by Patankar [22]. The discretization technique is well-known and only a brief description is given hereafter.

Discrete temperature, concentration and pressure values are computed at the nodes of a computational grid defined on the two-dimensional rectangular domain, while the velocity components are calculated at the nodes of two staggered subgrids. The conservation equations are integrated over the corresponding control volumes, leading to a local balance of the fluxes through the surfaces of the volume. The integrated equations are discretized using a combination of the centred and upwind schemes, according to the value of the local mesh Peclet number (the hybrid scheme of Patankar [22]). At a given iteration, the set of linear discretized equations derived from each conservation equation is solved using an ADI procedure, allowing for the use of fast algorithms to solve the tridiagonal systems.

As the momentum equation is formulated in terms of the primitive variables (velocity components and pressure) the iterative procedure includes a pressure correction method to solve the pressure–velocity coupling. The code uses a combination of alternatives to the initial SIMPLE algorithm (SIMPLER [22] and SIMPLEC [23]): the velocity correction step in the SIMPLER algorithm uses the SIMPLEC formulation. The numerical results presented in this paper have been obtained on a VP200 or a Cray-C98 vectorial computer, and an excellent vectorization level of the code has been achieved (see ref. [24]).

Table 1. Steady-state natural convection: comparison with the reference solution

Rayleigh number		Present work	De Vahl Davis [25]
10^5	ψ_{max}	9.590	9.644
	Nu	4.524	4.514
10^6	ψ_{max}	16.976	16.960
	Nu	8.815	8.798
	Grid	64×64 (Irregular)	81×81 (Regular)

The convergence criterion is based on two conditions:

(1) The ratio of the pressure correction term to the calculated local pressure. The maximum value of this ratio over the whole domain has to be less than a prescribed value, ε_1, generally 10^{-4}, then the continuity equation is supposed to be satisfied;

(2) The residues of the different conservation equations have to be less than ε_2, generally 10^{-6}, then the solution is considered to be converged.

The validity of the code has been assessed through a set of numerical tests and comparisons with published numerical results concerning natural thermal convection. The steady-state results have been compared (see Table 1) to the reference solution proposed by de Vahl Davis [25] for air in a square cavity. In the transient regime, the validation is based on the frequency of the stream function oscillations at the central point of the enclosure. At $Ra = 10^6$, the present code leads to a frequency of 85.7 on a 45×45 geometrical mesh, to be compared to the value proposed by Lauriat and Altimir [26] (86.9) using the SADI method, or by Le Quéré [27] (86.9) using a spectral method. Numerical solutions obtained with the hybrid scheme have been compared with calculations using a second-order upwinding scheme (QUICK [28]), especially when multicellular regimes are found, and no significant difference has been shown on the flow structure [29]. A detailed comparison with the experimental results for thermal convection near the density maximum of aqueous solutions is available [30].

4.2. *Numerical results*

The set of numerical simulations that is presented in this section has been performed in order to study the influence of the different dimensionless parameters, and to verify the orders of magnitude deduced from the above scaling analysis. In order to reduce the number of simulations, the range of variation of some parameters is limited, and only the cooperating situation ($N > 0$) is investigated. Moreover, this study is motivated by the analysis of thermosolutal effects on the phase change process of aqueous solutions: the Prandtl number is fixed to the

average value of water ($Pr = 7$) and the range of Lewis number is $Le > 1$. Finally, square cavities are considered ($A = 1$).

Thus, the steady-state solutions calculated in this parametric study are obtained over a range of thermal Grashof numbers, for positive buoyancy numbers and Lewis numbers larger than unity

$$\begin{cases} A = 1 \\ Pr = 7 \\ Gr_T \in [10^3\text{–}10^6]. \\ N \in [0.1\text{–}100] \\ Le \in [1\text{–}1000] \end{cases} \quad (27)$$

For each value of Gr_T (10^3, 10^4, 10^5, 10^6), N takes the values 0.1, 0.5, 1, 5, 10, 50 and 100, and the Lewis number is 1, 10, 100 and 1000. Let us mention that, for given values of Le and N, results in the $Le < 1$ range at $1/Le$ and $1/N$ may be deduced from those calculations by exchanging the role of the Nusselt and Sherwood numbers.

The discretization mesh used in these computations is irregularly spaced and the node spacing is increasing geometrically from the walls to the centre of the enclosure, so that at least three to four nodes are present in the thin solutal boundary layer. Obviously, the number of nodes has to be increased with increasing Le or N, and the most extreme situation is met for $Le = 1000$ and $N = 100$ ($Pr = 7$ and $Gr_T = 10^6$), which corresponds to a solutal Rayleigh number of order 10^{11}. Our analysis is limited to the study of laminar flows, and it is important to verify whether such high values may be considered. According to Bejan and Lage [31], the transition to the turbulent regime for natural convection in enclosures depends on the value of the Grashof number, and occurs for Gr of the order of 10^8. This is confirmed by the simulations by Brenier [32] at $Pr = 1000$, showing the transition at $Gr \geqslant 10^8$. The highest value considered in this study corresponds to a solutal Grashof number of 10^8, and the assumption of laminar flow may still be used.

The following sections are dedicated to the analysis of the influence of Gr_T, N and Le on mass transfer over this range of parameters. The heat transfer characteristics and the fluid flow structures are analysed in the companion paper.

4.2.1. *Influence of the buoyancy ratio* (N). Figure 4 displays the values of the Sherwood number $\overline{Sh}$ as a function of N. Each curve corresponds to a given value of the thermal Grashof number. This graph is obtained for $Le = 100$. It may be noted that the Sherwood number is roughly constant for low values of N: the thermal buoyancy term is then dominant, and the influence of the solutal force is negligible. At higher values of N, however, the Sherwood number is significantly increasing, and the variation of $\overline{Sh}$ is found to be of order $N^{1/4}$, which agrees well with our analysis, and with the experimental results by Kamotani *et al.* [6].

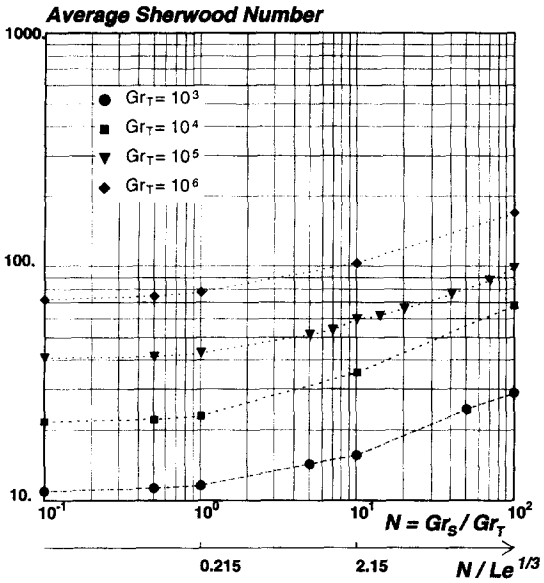

Fig. 4. Influence of N on mass transfer ($A = 1$; $Pr = 7$; $Le = 100$).

Our results also show that the transition between both regimes occurs for $N/Le^{1/3} \approx 1$ (Fig. 4). This excellent agreement with the orders of magnitude derived in the previous section has to be confirmed by the study of the influence of the Lewis number.

4.2.2. *Influence of the Lewis number* (Le). The results at a given thermal Grashof number $Gr_T = 10^5$ are represented in Fig. 5, where $\overline{Sh}$ is displayed as a function of the Lewis number, for different values of the buoyancy ratio. Again, two behaviours may be observed:

(1) For $N \leqslant 1$, the curves are superimposed, showing that the Sherwood number is globally insensitive

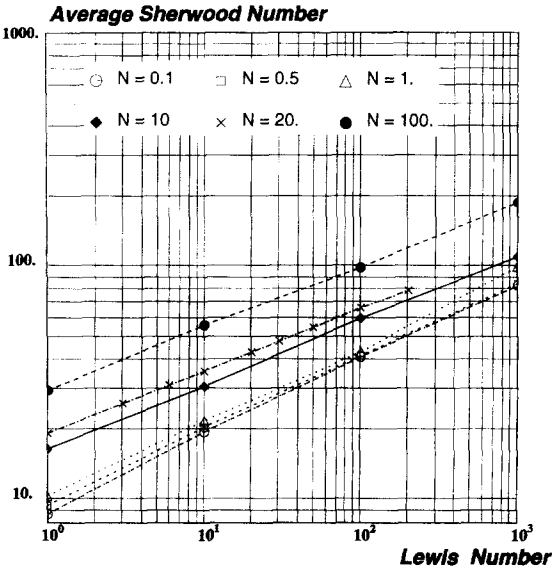

Fig. 5. Influence of Le on mass transfer ($A = 1$; $Pr = 7$; $Gr_T = 10^5$): $N = 0.1$; 0.5; 1; 10; 20; 100.

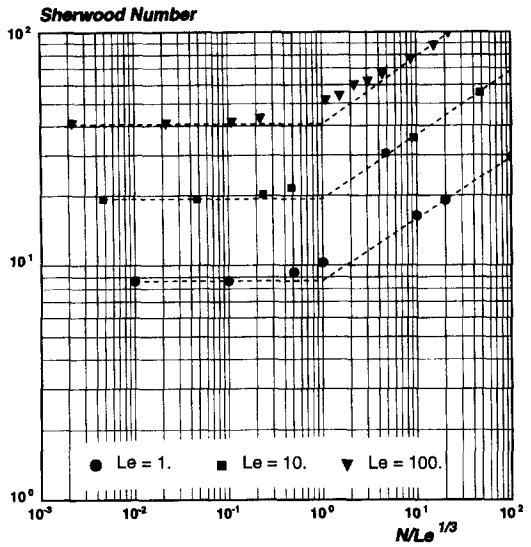

Fig. 6. Effect of $N/Le^{1/3}$ on mass transfer ($A = 1$; $Pr = 7$; $Gr_T = 10^5$).

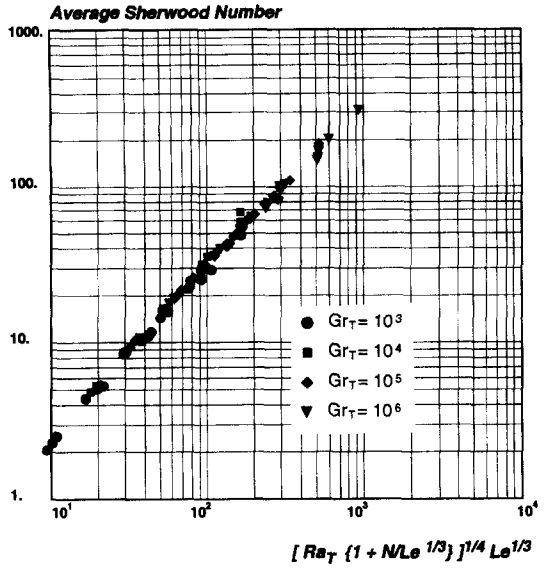

Fig. 7. Mass transfer at the vertical wall as a function of the dimensionless group arising from the scaling analysis.

to N. This is due to the fact that the flow is dominated by the (unchanged) thermal buoyancy term. However, $\overline{Sh}$ increases with the Lewis number (the solutal Rayleigh number is increasing through Le).

(2) For higher values of N, the solutal component of the buoyancy term becomes dominant enough ($N/Le^{1/3} > 1$) to modify the flow on the scale of the solutal boundary layer, and $\overline{Sh}$ increases with N.

Figure 6 gives the ($\overline{Sh}-N/Le^{1/3}$) representation of the results at $Gr_T = 10^5$, for different values of the Lewis number. The three distinct curves, corresponding to $Le = 1$, 10 and 100, show that there is a strong influence of the Lewis number on the level of mass transfer. But the transition from the heat transfer driven regime (constant $\overline{Sh}$) to the mass transfer driven regime ($\overline{Sh}$ proportional to $N^{1/4}$) appears clearly on the figure to occur for $N/Le^{1/3}$ of order 1, as predicted by our analysis.

Finally, the mass transfer variation with the Lewis number is different in each domain. At low values of $N/Le^{1/3}$, the scaling laws indicate that the Sherwood number varies as $Le^{1/3}$, while at high values of N, the variation is closer to the $Le^{1/4}$ law predicted by Bejan [19] [equation (19)]. This influence of the Lewis number has been confirmed by a more detailed set of simulations at a given value of N in the regime where the flow is driven by the solutal buoyancy force ($N = 20$ and $Gr_T = 10^5$).

4.3. *Sherwood number correlation*

We now wish to present all the numerical results as a function of a dimensionless group which might translate the asymptotic behaviours that we have observed in this study. This correlation would express the mass transfer variations as a function of the thermal Grashof number, as well as of the buoyancy ratio and of the Lewis number over the whole range of interest. The final correlation which satisfies the limiting behaviours, taking account of the scaling analysis, would be of the general form

$$\overline{Sh} \sim \left[Gr_T\left(1+\frac{N}{Le^{1/3}}\right)\right]^{1/4} Le^{1/3}. \qquad (28)$$

Such a representation is given in Fig. 7, where it may be seen that the main trends of the scaling analysis are remarkably verified by the calculations, and that all the numerical results cluster on a straight line with a relatively low dispersion.

The best fit of our numerical results leads to the expression

$$\overline{Sh} \sim \left[Gr_T\left(1+\frac{N}{Le^{0.29}}\right)\right]^{11/40} Le^{0.34}. \qquad (29)$$

In this correlation, the different exponents have been identified from regressions and the values are in fairly good agreement with the scaling laws. Extra calculations have been performed to show the sensitivity of the results to the Prandtl number ($Pr = 0.7$ and 70). As expected, the results show that for all the triplets (N, Le, Gr_T), the evolution of the mass transfer with Pr fits $\overline{Sh} \sim Pr^{1/4}$. Finally, the numerical results lead to a correlation which is valid on the whole range defined at the beginning of this section

$$\overline{Sh} = 0.2\left[Ra_T\left(1+\frac{N}{Le^{0.29}}\right)\right]^{11/40} Le^{0.34} \qquad (30)$$

for $A = 1$, $Pr > 1$, $Gr_T \in [10^3-10^6]$, $N \in [0.1\text{–}100]$, $Le \in [1\text{–}1000]$. The agreement with the numerical results is not so good for the lowest values of the equivalent Rayleigh number ($Ra_{eq} = Ra_T(1+N/Le^{0.29})$), where the difference is about 10% due to the

fact that the boundary layer approximation is not adapted any more.

4.4. *Comparison with previous results*

As mentioned in the introduction, the comparison of the present results with published data is limited to a narrow range of parameters, essentially because most results in the bibliography have been obtained for the situation where $Le = 1$, in spite of its restricted interest.

4.4.1. *Comparison at* Le = 1. In this situation, heat conduction and molecular diffusion are identical, and the flow is the same as a purely thermal natural convection flow, with an equivalent Rayleigh number resulting from the addition of the thermal and solutal Rayleigh numbers. A simplified form of the present correlation may be compared to the expressions previously established in refs [10 and 14]

Present Work (numerical, $A = 1$):

$$\overline{Sh} = \overline{Nu} = 0.2\,[Ra_T(1+N)]^{11.40}$$

Béghein *et al.* (numerical, $A = 1$) [14]:

$$\overline{Sh} = \overline{Nu} = 0.22\,[Ra_T(1+N)]^{0.27}$$

Trevisan and Bejan (analytical) [10]:

$$\overline{Sh} = \overline{Nu} = 0.34\,[Ra_T(1+N)]^{2.9}.$$

The results are compared in Fig. 8. A very good agreement is achieved with the numerical results proposed by Béghein *et al.* [14], while the agreement with the expression proposed by Trevisan and Bejan [10] is still satisfactory, since it has been theoretically obtained using an Oseen linearization technique.

4.4.2. *Comparison at* Le > 1. In the domain of very large Lewis numbers, it has been shown from the analysis of the *orders of magnitude* characterizing the boundary layer in a semi-infinite medium that for $N/Le^{1/3} \ll 1$, $\overline{Sh} \sim Ra^{1/4}Le^{1/3}$, and, for $N/Le^{1/3} \gg 1$, $\overline{Sh} \sim (Ra\,N\,Le)^{1/4}$.

Numerically we find, for the square cavity for $N/Le^{0.29} \ll 1$, $\overline{Sh} \sim Ra^{11/40}Le^{0.34}$, for $N/Le^{0.29} \gg 1$, $\overline{Sh} \sim (Ra\,N)^{11/40}Le^{0.26}$.

The *experimental* results of Kamotani *et al.* [6] at $Pr = 7$, $Le = 300$ and $N > 3.84$ give

$$\overline{Sh} = 0.67Le^{3/8}\left[Ra_T\left(1+\frac{N}{Le^{1/2}}\right)\right]^{1/4}$$

for $N/Le^{1/2} \ll 1$: $\overline{Sh} \sim Le^{3/8}Ra^{1/4}$ and for $N/Le^{1/2} \gg 1$: $\overline{Sh} \sim Le^{1/4}(Ra\,N)^{1/4}$.

This result confirms the existence of two distinct regimes, and that the condition is expressed in terms of the order of magnitude of the group N/Le^k compared to unity. The main limitation of this experimental result comes from the fact that the sensitivity to the Lewis number cannot be studied.

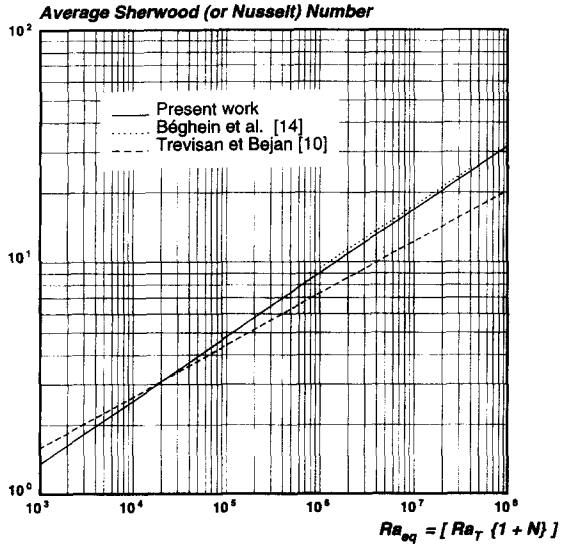

Fig. 8. Comparison between the existing correlations for the average wall Sherwood number ($Le = 1$).

5. CONCLUSION

This study is concerned with mass transfer due to thermosolutal natural convection with cooperating thermal and solutal buoyancy forces ($N > 0$). In terms of mass transfer, the numerical results are in good agreement on a wide range of Le and N with the orders of magnitude that can be deduced from a scaling analysis based on the boundary layer approximation along a vertical plate.

We have shown, and numerically verified, that the distinction between heat transfer driven flows and mass transfer driven flows is dependent on different criteria which are expressed in terms of N/Le for heat transfer, and of $N/Le^{1/3}$ for mass transfer. So, the scale on which the buoyancy forces act on the flow is of the same importance as the relative intensity of the thermal and solutal forces.

Finally, a general expression for the Sherwood number as a function of the main parameters of the problem is proposed over a very wide range.

Acknowledgements—The calculations have been performed on the C98 Cray supercomputer at IDRIS (the CNRS Computer Center in Orsay), in the frame of project #94-0336. The authors wish to gratefully thank J.-M. Teuler for his participation in the vectorization of the code, and C. Bénard for her helpful contribution in the analysis of the results.

REFERENCES

1. C. F. Chen and D. H. Johnson, Double diffusive convection: a report on an engineering foundation conference, *J. Fluid Mech.* **138**, 405–416 (1984).
2. D. A. Saville and S. W. Churchill, Simultaneous heat and mass transfer in free convection boundary layers, *AIChE J.* **16**, 268–273 (1970).
3. B. Gebhart and L. Pera, The nature of vertical natural convection flows resulting from the combined buoyancy effects of thermal and mass diffusion, *Int. J. Heat Mass Transfer* **14**, 2025–2050 (1971).

4. A. Bejan, *Convection Heat Transfer*. Wiley, New York (1984).
5. J. A. Weaver and R. Viskanta, Natural convection in binary gases due to horizontal thermal and solutal gradients, *J. Heat Transfer* **113,** 141–147 (1991).
6. Y. Kamotani, L. W. Wang, S. Ostrach and H. D. Jiang, Experimental study of natural convection in shallow enclosures with horizontal temperature and concentration gradients, *Int. J. Heat Mass Transfer* **28,** 165–173 (1985).
7. J. Lee, M. T. Hyun and K. W. Kim, Natural convection in confined fluids with combined horizontal temperature and concentration gradients, *Int. J. Heat Mass Transfer* **31,** 1969–1977 (1988).
8. H. Han and T. H. Kuehn, Double diffusive natural convection in a vertical rectangular enclosure. Part I: experimental study, Part II: numerical study, *Int. J. Heat Mass Transfer* **34,** 449–460, 461–471 (1991).
9. L. W. Wang and P. C. Chang, Flow patterns of natural convection in enclosures with horizontal temperature and concentration gradients, *Proceedings of the 8th Int. Heat Transfer Conf.* San Francisco, Vol. 4, pp. 1477–1481 (1986).
10. O. V. Trevisan and A. Bejan, Combined heat and mass transfer by natural convection in a vertical enclosure, *J. Heat Transfer* **109,** 104–112 (1987).
11. P. Ranganathan and R. Viskanta, Natural convection in a square cavity due to combined driving forces, *Numer. Heat Transfer* **14,** 35–59 (1988).
12. C. Bénard, D. Gobin and J. Thévenin, Thermosolutal natural convection in a rectangular enclosure: numerical results, *Heat Transfer in Convective Flows ASME National Heat Transfer Conf.*, Philadelphia, pp. 249–254. ASME, New York (1989).
13. J. W. Lee and J. M. Hyun, Double-diffusive convection in a rectangle with opposing horizontal gradients of temperature and concentration, *Int. J. Heat Mass Transfer* **33,** 1619–1632 (1990).
14. C. Béghein, F. Haghighat and F. Allard, Numerical study of double-diffusive natural convection in a square cavity, *Int. J. Heat Mass Transfer* **35,** 833–846 (1992).
15. W. Shyy and M. H. Chen, Double-diffusive flow in enclosures, *Phys. Fluids A* **3,** 2592–2607 (1991).
16. H. D. Jiang, S. Ostrach and Y. Kamotani, Unsteady thermosolutal transport phenomena due to opposed buoyancy forces in shallow enclosures, *J. Heat Transfer* **113,** 135–140 (1991).
17. J. W. Lee and J. M. Hyun, Time-dependent double diffusion in a stably stratified fluid under lateral heating, *Int. J. Heat Mass Transfer* **34,** 2409–2421 (1991).
18. G. Gau, K. H. Wu and D. J. Jeng, Layer growth process of transient thermosolutal convection in a square enclosure, *Int. J. Heat Mass Transfer* **35,** 2257–2269 (1992).
19. A. Bejan, Heat and mass transfer by natural convection in a vertical cavity, *Int. J. Heat Fluid Flow* **6,** 149–159 (1985).
20. C. Allain, M. Cloitre and A. Mongruel, Scaling in flows driven by heat and mass convection in a porous medium, *Europhys. Lett.* **20,** 313–318 (1992).
21. R. H. Nilson, Countercurrent convection in a double-diffusive boundary layer, *J. Fluid Mech.* **160,** 181–210 (1985).
22. S. V. Patankar, *Numerical Heat Transfer and Fluid Flow*. Hemisphere, New York (1980).
23. J. P. Van Doormaal and G. D. Raithby, Enhancements of the SIMPLE method for predicting incompressible fluid flows, *Numer. Heat Transfer* **7,** 147–163 (1984).
24. D. Gobin and M. Zarea, Transient thermosolutal natural convection in enclosures, *2nd Int. Conf. on Advanced Computer Methods in Heat Transfer*. Milano, Vol. 2, pp. 91–108, July (1992).
25. G. de Vahl Davis, Natural convection of air in a square cavity: a benchmark numerical solution, *Int. J. Numer. Meth. Fluids* **3,** 249–264 (1983).
26. G. Lauriat and I. Altimir, A new formulation of the SADI method for the prediction of natural convection flows in cavities, *Comput. Fluids* **13,** 141–155 (1985).
27. P. Le Quéré, Etude de la transition à l'instationnarité des écoulements de convection naturelle en cavité verticale differentiellement chauffé par méthode spectrale Chebyshev, Thèse d'Etat. Université de Poitiers (1987).
28. B. P. Leonard, A stable and accurate convective modelling procedure based on quadratic upstream interpolation, *Comput. Meth. Appl. Mech.* **19,** 59–98 (1979).
29. S. Belharat, Convection naturelle thermosolutale: mise en oeuvre du schéma QUICK, Internal Report (1994).
30. R. Bennacer, Convection naturelle thermosolutale: simulation numérique des transferts et des structures d'écoulement, Doctorat de l'Université Pierre et Marie Curie (1993).
31. A. Bejan and J. L. Lage, The Prandtl number effect on the transition in natural convection along a vertical surface, *J. Heat Transfer* **112,** 787–790 (1990).
32. B. Brenier, Développement d'une méthode Tau–Chebyshev pour l'étude des instabilités hydrodynamiques et thermiques dans une couche fluide, Thèse d'Université, Aix-Marseille II (1982).